

FAILURE OF UNS N10276 REACTOR IN SUPERCRITICAL WATER SERVICE

D. W. Alley, S. A. Bradley
UOP
25 E. Algonquin Rd.
Des Plaines IL 60017

ABSTRACT

Catalytic reactions in supercritical water represent a potential alternative to conventional hydroprocessing of heavy oils. A pilot plant with a reactor constructed from UNS N10276 was developed to test this possibility. Rapid failure of the reactor due to intergranular corrosion was observed in the reactor at a point where the temperature of the water feed was in the high subcritical range. The cause for the corrosion was not determined, however, it appears to be related to a proprietary carbonate in the water feed.

Keywords: supercritical water, corrosion, UNS N10276, heavy oils, stainless steel

INTRODUCTION

Supercritical fluids, and supercritical water in particular, have become important commercial tools for chemical extractions and reactions in many industries. No attempt will be made here to cover the breadth of this subject. In the hydrocarbon processing industry significant interest, although little or no commercial success, has been expressed in the use of supercritical fluids for heterogeneous catalysis.¹⁻² The use of supercritical water oxidation for hydrocarbon processing,^{3,4} particularly the hydrodesulfurization of dibenzothiophene⁵, hydrogenation of hydrocarbons⁶ and the hydrodesulfurization and demetalization⁷ of gasoil has been described.

Based on the above work, it appears that supercritical water may be effective in the hydrodesulfurization and demetalization of heavy oils including vacuum gas oil and resid. These oils represent the high boiling fractions from the distillation of crude oil. They are of low value when compared to lighter products for a variety of reasons including high metal and sulfur content. High sulfur content, typically requires the use pollution control devices to reduce sulfur emissions if these oils are used as fuels without further treatment. High metal contents, particularly vanadium, can result in accelerated corrosion of heat exchanger tubes through the formation of low melting point vanadates.⁸ Currently, a significant percentage of

the oils of this type receive further treatment to enhance their value. These oils may be hydrocracked to reduce sulfur and molecule size or they may be hydrotreated to reduce sulfur. Both of these processes involve high temperatures and pressures in a corrosive environment. As a result, both processes are costly from both a capital and operational perspective. An alternate means of desulfurizing and demetallizing heavy oils could provide significant economic benefit to refiners.

As is the case in the development of any new process, a literature search was conducted to determine the appropriate materials of construction for the experimental equipment. This search was somewhat less helpful than desired as no information was found concerning flowing systems containing heavy hydrocarbons and supercritical water. Some information was identified for systems that were related to the proposed experimental system.

Two bodies of work have considered hydrocarbon environments which are somewhat similar to the one under consideration. Arai⁶ studied heavy hydrocarbons in supercritical water. His work involved very short duration tests (less than 1 hour) in autoclaves. He did not report experiencing any corrosion problems. McKay⁹ investigated the ability of a supercritical solution of 50% water 50% methanol to extract oil from the Green River Oil Shale. His experiments were relatively short, less than three hours, and were conducted in a 20Cb3 autoclave. He also did not report experiencing any corrosion problems.

Contrary to the two previous two studies, Downey¹⁰ found corrosion rates to be exceptionally high in systems designed for the destruction of nerve gases (GB, VX, and mustard). These gases break down to hydrofluoric, hydrochloric, sulfuric, and phosphoric acids. In order to be commercially practical, the concentration of the nerve gases being destroyed, and therefore the acids, must be high. As a result, the corrosive environment in these tests was very severe. Corrosion testing was conducted in a platinum lined flow reactor because standard materials of construction were deemed inadequate for even short term testing. Most materials tested experienced corrosion rates in excess of 200 mpy. Platinum had acceptable corrosion rates (<10 mpy) in non-HCl containing environments. In HCl-containing environments, platinum corroded at over 200 mpy at temperatures just below critical. The corrosion rate declined with increasing temperature.

The most applicable body of work to the proposed experimentation was conducted at MIT.¹¹⁻¹³ These studies indicated that UNS N10276 is subject to very rapid corrosion (850 – 2000 mpy) when exposed to dichloromethane (CH₂Cl₂) and water environments at supercritical pressures and temperatures just below supercritical. The corrosion rates of the same mixture at lower temperatures as well as supercritical temperatures was found to be much lower. The corrosivity in the environment was thought to be due to the breakdown of the dichloromethane to HCl. This unit had performed satisfactorily for 10 years in non-chlorinated hydrocarbon service before the rapid failure in dichloromethane. Corrosion testing of pure supercritical water revealed some, but not excessive corrosion of nickel based alloys. The authors resolved the dichloromethane corrosion problem by delaying the mixing of the water and dichloromethane until they had reached supercritical conditions.

EXPERIMENTAL

Reactor Construction

Based on the results of the literature search summarized above, the reactor, part of which is shown in Figure 1, was constructed. It must be remembered that the purpose of this device was process testing rather than corrosion testing. As a result, instrumentation was not ideal for a corrosion experiment. The findings from the MIT work regarding corrosion of UNS

N10276 by HCl solutions at slightly subcritical conditions were followed closely in the design of the apparatus. Since the oils being tested in this work may contain chlorides, the apparatus was designed specifically to ensure that the oil and water mixed only after they reached supercritical temperatures.

While the entire experimental setup is somewhat complex, from a corrosion perspective there are three components of interest; all are contained within the reactor. These are the reactor, the dip tube, and the tripod.

The reactor is a 45 ¼" long section of 1" schedule 160 UNS N10276 pipe which is threaded on both ends. Since this reactor had been previously used in other services, it was carefully inspected both visually and ultrasonically prior to being placed in service. Wall thickness throughout the length of the pipe was found to be 0.25" which corresponds to the "as new" condition. Visual inspection revealed no defects.

The dip tube is a 19" long section of ¼" UNS N10276 tubing. The dip tube is radially centered within the reactor. The dip tube is held in place by the bottom head of the reactor and the tripod. Oil flows within the dip tube while water flows in the annular space surrounding it.

The tripod is a device present within the reactor for the sole purpose of supporting the dip tube. It was constructed of type 316 stainless steel. This metallurgy was based on convenience rather than corrosion considerations. The tripod is approximately 19" long.

As is shown in Figure 1, oil enters from the bottom of the reactor within the dip tube. Oil pressure at this point exceeds the critical pressure of water but the temperature does not. The exact critical temperature and pressure for the oil and oil water mixture were not determined. Water also enters the reactor from the bottom in the annular space surrounding the dip tube. It also has sufficient pressure but insufficient temperature to be supercritical. As the water and oil travel up the dip tube and the annular space they acquire heat from the reactor's external heat source. The exact temperature profile is not known in this section of the reactor. It is known that the temperature exceeds that which is necessary to form supercritical water at some point prior to the mixing zone, based on readings from a thermocouple in the mixing zone.

Feed

The composition of the oil feed is shown in Table 1. The sulfur content of this feed is fairly typical, while the metals content is rather low. The chloride content of the oil feed was not measured, however, the presence of chlorides in this type of oil should be expected.

The basis for the water feed was high purity deionized water. As such, no chlorides were expected in the water. Low levels of a proprietary carbonate were included in the water feed

The ratio of oil to water fed was 1:1.

Failure

Two runs were conducted in the apparatus. The first run was halted after 3 hours due to a leak in the reactor outlet piping. This leak was mechanical in nature and not related to corrosion. The second run, planned to last 24 hours, was successfully completed. Following the completion of the run, hydrogen was substituted for the feed and the reactor was allowed to cool while system pressure was maintained. During the period after the reactor reached room temperature and while pressure was being reduced (pressure was still in excess of 2000

psi), smoke was observed coming from beneath the reactor heating equipment. The system was then depressurized, and all the equipment external to the reactor was removed. The system was then pressure tested. During the pressure test, several leaks were observed. The reactor was then removed for a complete metallurgical failure analysis.

FAILURE ANALYSIS

Visual Analysis

The reactor was received with the location of the holes detected via the pressure test marked. As shown in Figure 2, the locations of the preheat zone (labeled water only), the mixing zone, and the reaction zone were marked to orient the remainder of the investigation. As may be seen from this Figure, there is little evidence of corrosion from the outside of the reactor.

Following the external visual examination, the reactor was sectioned longitudinally. One section was subjected to dye penetrant examination. Dye penetrant revealed several cracks in the preheat zone and no cracks in the mixing or other zones. Some of the preheat zone cracks on the ID of the reactor are shown in Figure 3.

The dip tube and the tripod were also subjected to visual examination. Discoloration and increased surface roughness were detected in the preheat zone. Less evidence of attack was visible in the mixing zone and the lower temperature end of the preheat zone.

Chemical Analysis

Chemical analyses were conducted using energy dispersive spectroscopy (EDS), x-ray diffraction and inductively coupled plasma spectroscopy (ICP). Metallurgy of the reactor and internals was confirmed by ICP. EDS was conducted on the base metal, the surface corrosion scale within the mixing zone, the surface corrosion scale on the water side of the dip tube approximately 7 inches below the mixing zone, and on the deposits within the intergranular cracks found in the dip tube at the same location where the surface scale was measured. When interpreting these data it must be remembered that EDS is a semiquantitative method. Measured carbon and oxygen concentrations are generally higher than actual, due to the process of mount preparation. EDS results are provided in Table 2.

Approximate background levels of carbon and oxygen are represented by the carbon and oxygen levels for the base metal, i.e, the actual C and O levels in the base metal approach 0, so all the measured C and O represent background. From this it may be inferred that there is little or no carbon in the dip tube scale or cracks, as is expected from a surface exposed only to the water phase. There is substantial carbon in the scale from the mixing zone, as would be expected for a surface exposed to hydrocarbons. Significant oxygen is contained in all scales and cracks that are examined. Based on the ratios of Fe, Ni, Cr, and Mo in the base metal and in each of the measured scales and cracks, it does not appear that there is a significant enrichment or depletion of elements in the scale, except for a depletion of chromium in the mixing zone scale and a depletion of Mo in all the scales. Significant quantities of sulfur are observed in the mixing zone scale. Smaller quantities are observed in the dip tube scale. Essentially no sulfur is observed in the intergranular dip tube cracks.

As determined by x-ray diffraction, the crystalline components of the scale in the mixing zone are predominantly Ni_3S_2 with minor amounts of Fe_3O_4 and NiFe_2O_4 .

Metallographic Analysis

Sections were cut and polished at several locations. Micrographs of these samples are shown in Figures 4 - 13. The approximate location for these micrographs, relative to the point in the reactor at which oil and water mixed, may be found in Figure 1. It must be remembered that the water reached supercritical conditions at some point before the mixing point, however, the exact location is unknown. Furthermore, it is unclear whether the mixture of oil and water was supercritical after the fluids were mixed.

Figure 4 illustrates the condition of the inner surface of the alloy 276 reactor at the point of one of the through wall failures (approximately 8" below the mixing point.) Note the extensive intergranular corrosion.

Figure 5 illustrates the inner surface of the alloy 276 reactor at the same distance from the mixing point as Figure 4. Figure 5 is located on the opposite inner surface (approximately 180° from Figure 4. Even though there is extensive intergranular attack in this Figure, it is far less than that in Figure 4.

Figures 6 – 9 illustrate the condition of the outer surface of the dip tube (that exposed to the water) at 1, 3, 7, and 12 inches below the mixing point. Note the absence of significant intergranular attack in Figures 6 and 9, taken at 1 and 12 inches below the mixing point, and the significant attack shown in Figure 7 and 8 taken at 3 and 7 inches below the mixing point.

Figures 10 – 12 illustrate the condition of the tripod (type 316 stainless steel) at 3, 7, and 13 inches below the mixing point. Note that while all Figures show attack, the attack is substantially greater in Figure 11 which is at 7 inches below the mixing point.

Figure 13 illustrates the condition of the inner surface of the reactor in the mixing zone. Note the presence of minor intergranular attack.

Surfaces of the dip tube which were exposed to oil were examined; no corrosion was observed.

DISCUSSION

The information obtained from the metallographic analysis of the reactor, dip tube, and tripod appears to present a consistent picture regarding the corrosion of the experimental setup. The corrosion was observed only on those components exposed to water and was found to be intergranular in nature and highly sensitive to temperature. Given the approximate entry (in the range of 100°C) and mixing zone (in the range of 400°C) temperatures for the oil and water and assuming a linear variation of temperature within the reactor and dip tube, it appears that water side corrosion is minimal at substantially subcritical and supercritical temperatures and maximum at temperatures slightly below supercritical. Oil side corrosion prior to mixing is very low to non-existent and is independent of temperature.

The slight intergranular corrosion seen in the mixing zone is more difficult to interpret due to an increased number of variables. The most obvious change is that in the mixing zone the potentially corrosive environment consists of a solution of hydrocarbons and water. Slightly more subtle issues include the presence of chlorides and sulfur in the solution. Temperature may also be a significant issue. While it is certain that the temperature in the mixing zone is above that necessary for water to be supercritical, it is not known with certainty that the conditions in the mixing zone are supercritical for the solution. Past efforts to predict the critical properties of complex solutions using computer codes have proven unreliable and the experimentation necessary to verify supercritical conditions of the solution at this point in the reactor was not conducted. It is therefore possible that the corrosion observed in the

mixing zone was due to one or more of the following: the simple mixing of supercritical water phase and hydrocarbons; the addition of sulfur and/or chlorides to the water phase, including the potential for the formation of HCl; or that the solution was in the slightly subcritical temperature regime which proved to be very corrosive for the water phase. Further definition of the corrosion mechanism in the mixing zone will require additional experimentation.

Given the experimental similarity between this work and that conducted at MIT¹¹⁻¹³, it is interesting to compare the experimental conditions and corrosion results of these works. The corrosion results of the two bodies of work are essentially identical in overall results, i.e., in both works UNS N10267 failed due to extremely rapid intergranular corrosion at pressures above the critical point for water but temperatures slightly below the critical point.

Chemical analyses of the corrosion scales in the two works were somewhat more difficult to interpret. MIT results¹² revealed a selective dissolution of nickel by the corrosive medium, i.e., the ratio of Ni to Ni+Cr in the solution was greater than that in the alloy and the nickel concentration within the corrosion product was substantially reduced (as determined by augur line scan) as compared to the nickel concentration in the alloy. Augur line scan also indicated an enrichment of chromium and oxygen within the corrosion product as compared to the base metal. Chemical results in the present work, which were conducted by EDS and x-ray diffraction (see Table 2), show a depletion of Mo in all scales and a depletion of Cr in the mixing zone scale as compared to the base metal. While there are some variations in the scales between Fe and Ni, it is not clear that they are significant. X-ray diffraction, on the other hand, indicates that the scale in the mixing zone is predominantly Ni₃S₂ with minor amounts of Fe₃O₄ and NiFe₂O₄. Although EDS results are inconclusive, x-ray results in the present work concur with Mitton's¹² work regarding the importance of Ni to the corrosion process.

Levels of sulfur found in the mixing zone scale and in the dip tube cracks are as expected. Significant levels of sulfur, on the order of 5%, were found in the mixing zone scale. At this location, the sulfur may be attributed to the sulfur contained in the oil. Essentially no sulfur was detected in the dip tube cracks. This is also as expected since the cracks formed from the water side of the dip tube and should not have been exposed to oil. Of interest is the relatively low level of sulfur in the dip tube surface scale (0.34%). The sulfur content in the scale on the water side of the dip tube should have been zero as the sulfur containing oil should never have contacted this location. While the identification of sulfur at this location is unexpected, it is probably due to artifacts in sample preparation, such as smearing of sulfur bearing material across the (thin) surface of the tube from the oil contact (inner) surface to the water contact (outer) surface of the tube during the polishing process.

Despite the similarities in speed, location (temperature), appearance, and potentially, the chemistry of the corrosion products between the two bodies of work, the chemistry of the environments which created the corrosion was substantially different. Furthermore, the present experimental design was selected specifically to avoid the conditions (acid chloride selective dissolution of the grain boundaries) which Mitton¹² believed to be responsible for the failures. The belief that the failures experienced at MIT are due to acid chlorides (HCl) appears to be based on prior testing of various alloys in water systems at both sub and supercritical temperature as well as the successful operation of their test unit over many years with a mixture of water and non-chlorinated hydrocarbons.

For the present system it was decided to avoid any possibility of generating a solution of acid chlorides at slightly subcritical temperatures by not permitting the chloride containing oil to mix with the water until the water had reached a supercritical state. This was somewhat fortuitous since it would not have been possible to thoroughly mix the oil and water at a lower temperature. For catalytic reasons it was necessary to include a small concentration of carbonates to the feed water. Although experimentation to confirm the effect of these

materials on the corrosion of the reactor system was not conducted due to the cessation of work on the project, it appears highly probable that basic solutions as shown in equation 1



are capable of causing intergranular corrosion / stress corrosion cracking of UNS N10276. Although the mechanism has not been verified, it is theorized that the concentration of carbonate present in the water feed caused the system's electrochemical potential to shift to a point near the active/passive transition which resulted in rapid attack of the grain boundaries. This hypothesis is consistent with the mechanism attributed to intergranular alkaline stress corrosion cracking in aqueous environments.¹⁴

CONCLUSIONS

UNS N10276 is subject to intergranular corrosion / stress corrosion cracking at pressures above the critical point and temperatures slightly below the critical point when exposed to water containing low concentrations of carbonates. The rate of corrosion diminished very rapidly as temperature increased or decreased. Type 316 stainless steel was also subject to intergranular corrosion over a slightly wider temperature range however the most rapid corrosion also appeared to occur at a temperature slightly below critical. A slight amount of corrosion was observed after the water feed was mixed with vacuum gas oil at temperatures above the critical point of water. It is not clear whether this corrosion is due to the chloride content in the oil or an increase in the temperature required for the oil water mixture to be supercritical.

While the exact agent and mechanism for the rapid corrosion observed in the water feed environment are not known with certainty, based on other studies reported in the literature it appears doubtful that the water is responsible for the rapid corrosion. Since solutions of sodium hydroxide and sodium carbonate are known to cause intergranular cracking in aqueous systems by establishing a system potential near the passivating potential of the metal, there is a possibility that the concentration of carbonates in the water feed was sufficient to cause a similar potential, relative the passivating potential at slightly subcritical temperatures in the system under study. Additional work is required to clarify these issues.

REFERENCES

1. B. Subramaniam and M. A. McHugh, Reactions in supercritical fluids – a review, *Ind. Eng. Chem. Process Des. Dev.*, **25** (1986) p. 1-12.
2. B. Subramaniam, Continuous heterogeneous catalysis with near critical reaction media: fundamentals and reaction engineering aspects, *Proceedings of the 5th International Symposium on Supercritical Fluids, ISSF2000 [CD ROM]* (Georgia Institute of Technology, Atlanta Ga, 2000) p. 1
3. R. W. Shaw et. al., Supercritical water, a medium for chemistry, *C&EN*, **69** [51](1991) p. 26.
4. N. Akiya and P. E. Savage, Role of Water for Reactions in Supercritical Water, *Proceedings of the 5th International Symposium on Supercritical Fluids, ISSF2000 [CD ROM]* (Georgia Institute of Technology, Atlanta Ga, 2000) p.1
5. T. Adschiri et. al., Catalytic hydrodesulfurization of dibenzothiophene through partial oxidation and a water-gas shift reaction in supercritical water, *Ind. Eng. Chem. Res.*, **37** (1998) p. 2634-2638.

6. K. Arai, T. Adschiri, and M. Watanabe, Hydrogenation of hydrocarbons through partial oxidation in supercritical water, *Ind. Eng. Chem. Res.*, **39** [12] (2000) p 4697-4701.
7. B. M. Vogelaar, M. Makkee, and J. A. Moulijn, Applicability of supercritical water as a reaction medium for desulfurisation and demetallisation of gasoil, *Fuel Processing Technology*, **61** (1999) p, 265-277.
8. G. Y. Lai, *High-Temperature Corrosion of Engineering Alloys*, (ASM International, Metals Park OH, 1990) p. 43.
9. J. F. McKay, M. S. Blanche, Effect of time and pressure on recovery of oil from Green River oil shale in extraction experiments conducted at 400C, *Fuel Sci Tech Int.*, **4** [4] (1986) p. 413-431.
10. K. W. Downey et. al., Corrosion and chemical agent destruction research on supercritical water oxidation, *Innovation in Supercritical Fluids Science and Technology*, K. W. Hutchenson ed., American Chemical Society, Washington DC, 1995) p. 179-196.
11. P. A. Marrone et. al., CH₂Cl₂ oxidation and hydrolysis, *Innovation in Supercritical Fluids Science and Technology*, K. W. Hutchenson ed., American Chemical Society, Washington DC, 1995) p. 197-216.
12. D. B. Mitton, J. C. Orzalli, and R. M. Latanision, Corrosion studies in supercritical water oxidation systems, *Innovation in Supercritical Fluids Science and Technology*, K. W. Hutchenson ed., American Chemical Society, Washington DC, 1995) p. 327-347.
13. J. C. Orzalli, masters thesis, Massachusetts Institute of Technology, 1994.
14. J. E. Reinoehl and W. E. Berry, Natural conditions for caustic cracking of a mild steel, *Corrosion*, **28**, [4] (1972) p. 151-160

TABLES

Table 1 Feed Composition

Feed Properties	
API Gravity	23.2
Sulfur	2.21 wt %
Total Metals	0.825 wtppm
Bromine Number	2.0
Distillation	10% : 746.°F 50% : 837.°F 90% : 934.°F

Table 2 Avg. corrosion scale Composition via EDS

	Base Metal	Mix Zone	Dip Tube Scale	Dip Tube Crack
C	5.62	42.37	7.11	10.79
O	2.43	14.69	18.34	12.28
Mg	0.2	--	0.08	0.2
Al	0.26	0.08	0.31	0.26
Si	0	0.23	0.11	0
S	0	4.70	0.34	0
Cr	16.39	4.69	17.37	11.73
Mn	0.34	0.60	0.49	0.34
Fe	5.74	2.56	4.82	4.19
Ni	48.83	20.43	44.83	51.54
Mo	16.58	4.14	4.14	4.97
P	0	--	0.01	0
Ca	0.05	--	0.15	0.17
W	3.53	--	1.51	1.58

FIGURES

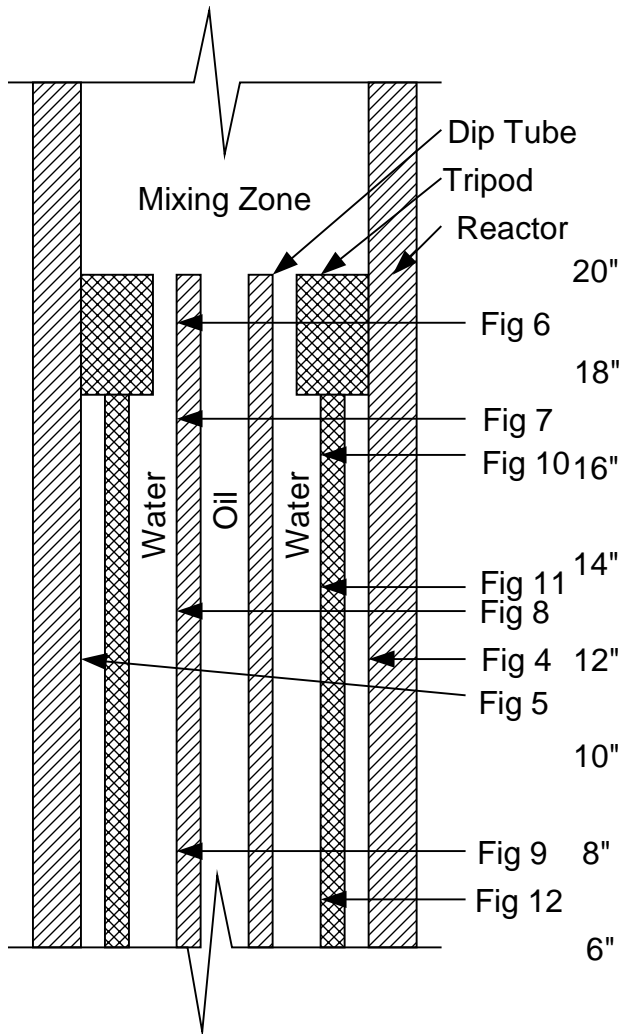


Figure 1 Schematic drawing of reactor and internals. Reactor, dip tube, and thermowell are alloy 276. Tripod is type 316 stainless steel

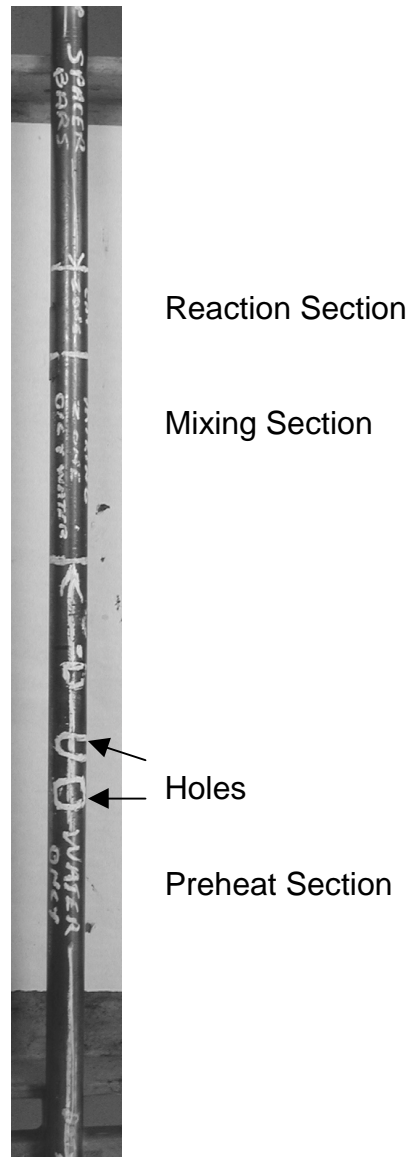


Figure 2 Photo of exterior of reactor. Location of holes detected by pressure test as well as preheat (water only), mixing and reaction zones are marked.

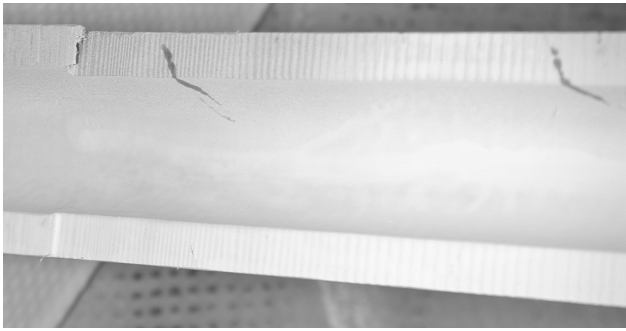


Figure 3 Photo of cracking on the ID of the reactor in the preheat zone revealed by dye penetrant examination

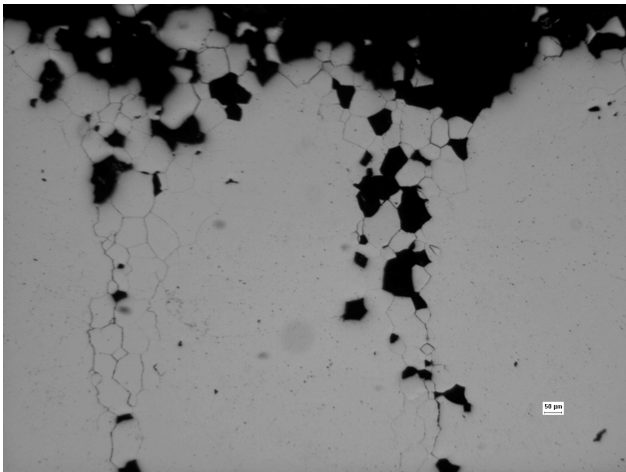


Figure 4 Micrograph of reactor ID at location of failure (approx. 8" from mixing zone)

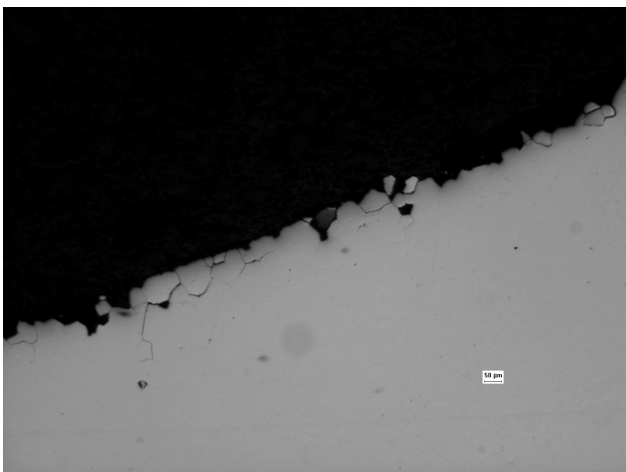


Figure 5 Micrograph of reactor ID 180° from Figure 4 at same distance from mixing zone

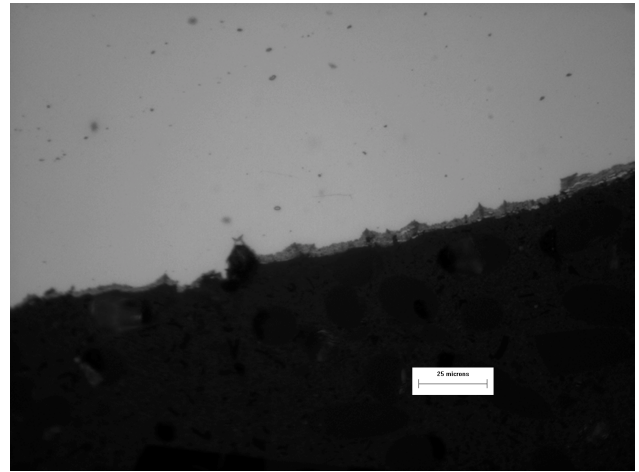


Figure 6 Micrograph of water side of dip tube 1" from mixing zone

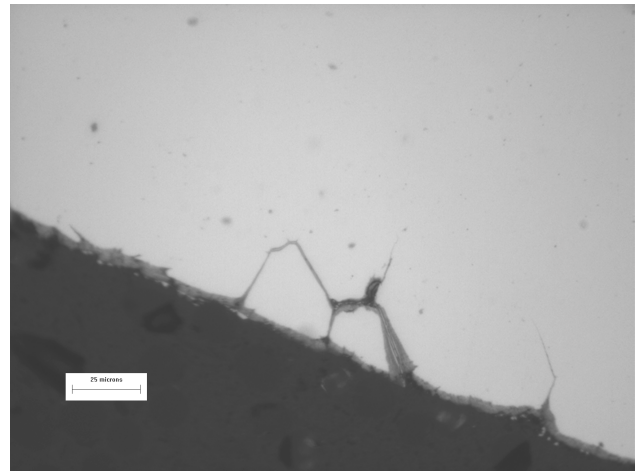


Figure 7 Micrograph of water side of dip tube 3" from mixing zone

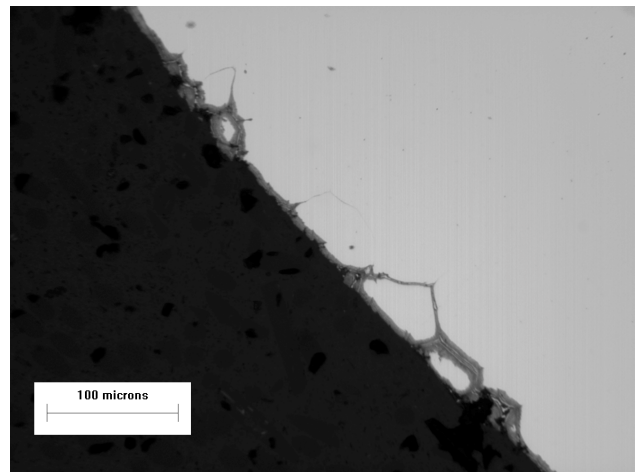


Figure 8 Micrograph of water side of dip tube 7" from mixing zone

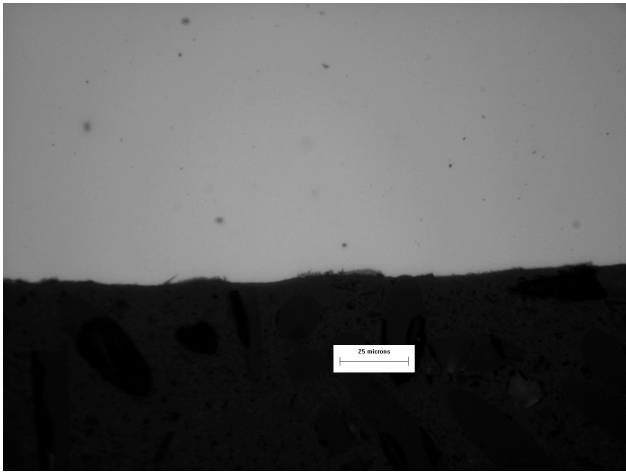


Figure 9 Micrograph of water side of dip tube 12" from mixing zone

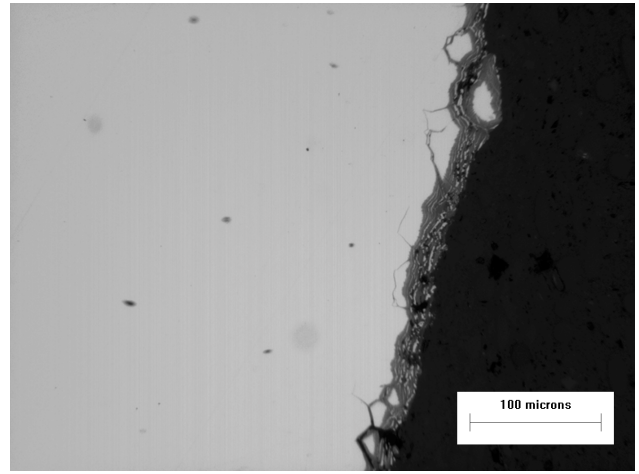


Figure 12 Micrograph of tripod 13" from mixing zone

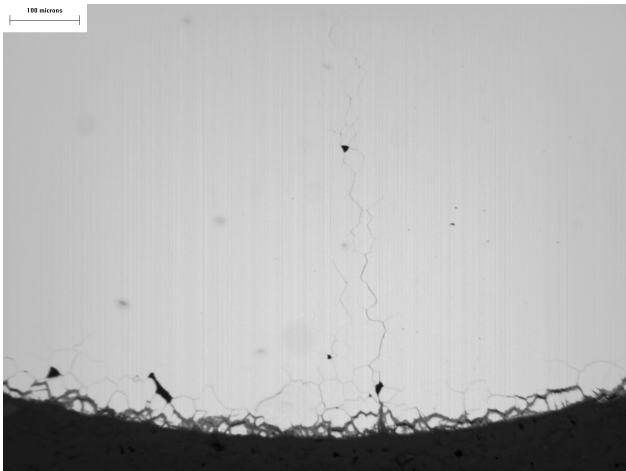


Figure 10 Micrograph of tripod 3.5" from mixing zone

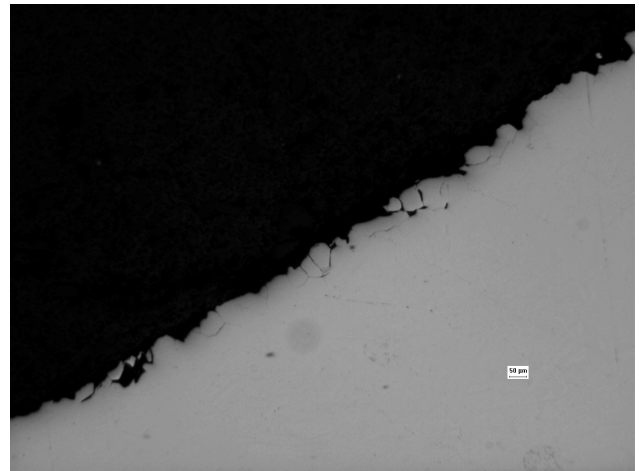


Figure 13 Micrograph of reactor ID in the mixing zone

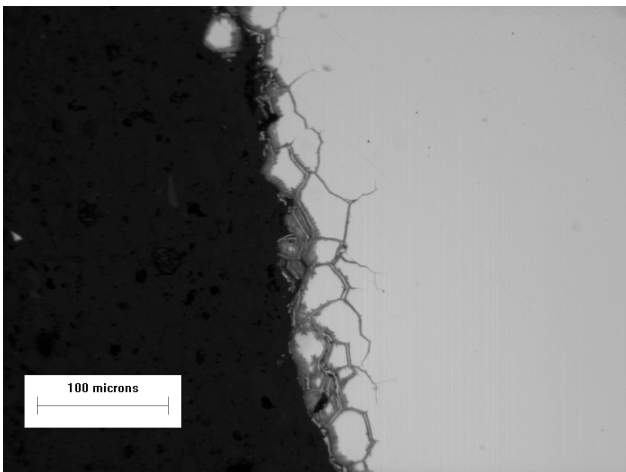


Figure 11 Micrograph of tripod 6.5" from mixing zone